Electronic Supplementary Material (ESI) for Journal of Materials Chemistry A.

Supplementary Information

Metal−Organic Cage with Light-Switchable Motifs for Controllable CO_2 Adsorption

Yao Jiang,[1†]* Tao Yang,[2†] Xiao-Qin Liu,[2] Peng Cui,[1] and Lin-Bing Sun[2]*

[1]*School of Chemistry and Chemical Engineering, Hefei University of Technology, Hefei 230009, China*

[2]*State Key Laboratory of Materials-Oriented Chemical Engineering, College of Chemical Engineering, Nanjing Tech University, Nanjing 211816, China*

*Corresponding authors. E-mail: yjiang@hfut.edu.cn; lbsun@njtech.edu.cn

Experimental Section

Chemicals

Bis(cyclopentadienyl)zirconium dichloride (Cp_2ZrCl_2; Aldrich, 98%), *N*, *N*-dimethylformamide (DMF; Aldrich, 99.8%), tetrahydrofuran (THF; 99.8%, Aldrich), methanol (MeOH; Aldrich, 99.5%). Other chemicals were purchased from Adamas-Beta and used directly without further purification. Deionized water was generated by a Milli-Q integral pure and ultrapure water purification system and used in all experiments in this work.

Materials synthesis

Synthesis of NUT-102

NUT-102 was synthesized by the solvothermal method. Cp_2ZrCl_2 (30 mg) and azo-H_2BDC (15 mg) were dissolved in a mixed solution of DMF (1 mL) and THF (0.5 mL) followed by the addition of deionized water (0.2 mL). The mixture was treated ultrasonically until all solids dissolved completely and kept at room temperature until the appearance of crystals. After that, the mother liquid was decanted and the resultant orange crystals were filtered and sequentially washed with DMF, THF, and dichloromethane. Finally, NUT-102 was obtained after vacuum drying at room temperature.

Characterizations

Single-crystal X-ray data was collected on a Bruker Smart APEX II CCD single-crystal diffractometer. The structure was solved by direct methods and refined by full-matrix least-squares on F2 with anisotropic displacement using the SHELXTL software package[1,2]. The

diffused electron densities resulting from these residual solvent molecules were removed from the data set using the SQUEEZE routine of PLATON and refined further using the data generated[3]. Matrix-assisted laser desorption/ionization time-of-flight mass spectrometry (MALDI-TOF-MS) were performed on an AB SCIEX 5800 instrument, and the regent of 2-cyano-3-(4-hydroxyphenyl)acrylic acid (CHCA) as the matrix during the experiments. Powder X-ray diffraction (PXRD) patterns of the materials were recorded with an X-ray diffractometer (Japan Rigaku D/MAX-γA) using Cu Kα radiation at 40 kV and 100 mA. Scanning electron microscopy (SEM) and corresponding elemental mapping analysis were performed using a Hitachi TM 3000 electron microscope operated at 2 kV. Fourier transform infrared (FT-IR) spectra of the samples diluted with KBr were carried out on a ThermoFisher Nicolet iS10 spectrometer with KBr wafer. UV/vis spectra were collected on the PerkinElmer Lambda 35 instrument. To study the light switchable property, the sample was dissolved in a solvent of ethylene glycol at a concentration 1 mg/5 mL. A xenon lamp (CEL-HXUV300) equipped with a filter was used as the UV/Vis source. X-ray photoelectron spectroscopy (XPS) was tested through a Thermo Scientific ESCALAB 250Xi spectrometer. Thermogravimetric analysis (TGA) curve was obtained by use of a thermobalance (STA-499C, NETZSCH). The sample was heated from room temperature to 1000 ºC with the heating rate 10 ºC·min^{-1} under a flow of nitrogen (10 mL·min^{-1}).

Adsorption tests

All adsorption isotherms were measured using an ASAP 2020 analyzer. Highly pure gases CO_2 (99.999%), CH_4 (99.999%), and N_2 (99.999%) were employed for the measurements. The

sample was degassed at 60 °C under vacuum for 12 h prior to adsorption analysis. A xenon lamp was used as the light source to generate lights with different wavelength. To investigate the adsorption selectivity of CO_2 over CH_4 or N_2 on the sample of NUT-102, the selectivity is defined as:

$$S = \frac{x_1 / y_1}{x_2 / y_2}$$

where x_1 and y_1 (x_2 and y_2) are the molar fractions of component 1 (component 2) in the adsorbed and bulk phases, respectively. The ideal adsorption solution theory (IAST) of Myers[4] has been reported to predict binary gas mixture adsorption in porous materials accurately, and the single-site Langmuir-Freundlich equation (LF) model was chosen to fit the adsorption isotherms, and then IAST was utilized to estimate CO_2/CH_4 or CO_2/N_2 selectivity of adsorbent. The isosteric adsorption heats (Q_{st}) of CO_2 was calculated from the adsorption isotherms at temperatures of 273 and 298 K, the data were simulated with Virial expression as below.

$$\ln P = \ln N + \frac{1}{T}\sum_{i=0}^{m} N^i + \sum_{i=0}^{n} b_i N^i$$

$$Q_{st} = -R\sum_{i=0}^{m} a_i N^i$$

where P is pressure, N is amount adsorbed, T is temperature, and m and n represent the number of parameters a and b ($m \leqslant 5$ and $n \leqslant 2$)

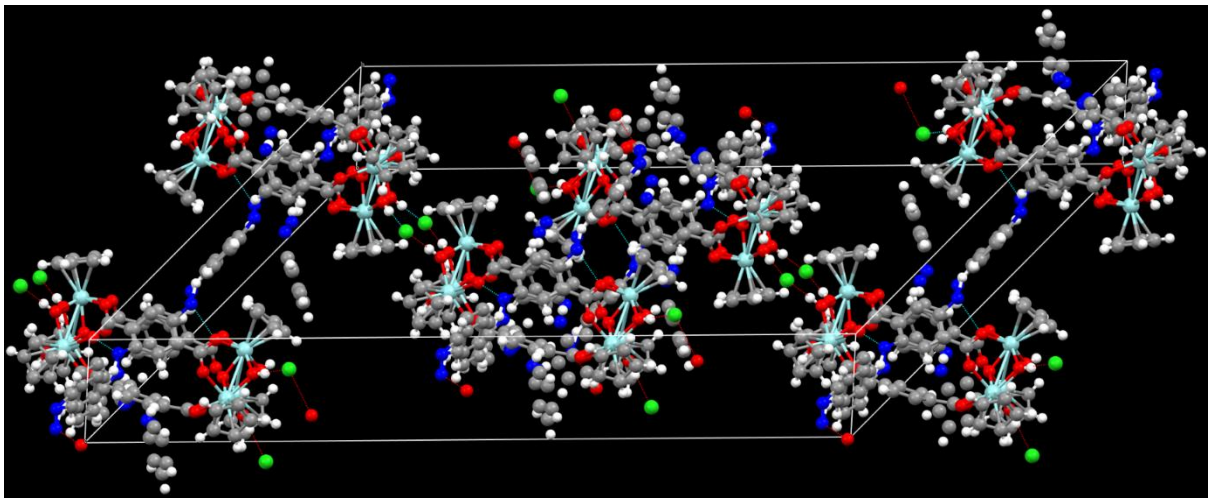

Figure S1. A unit cell of NUT-102.

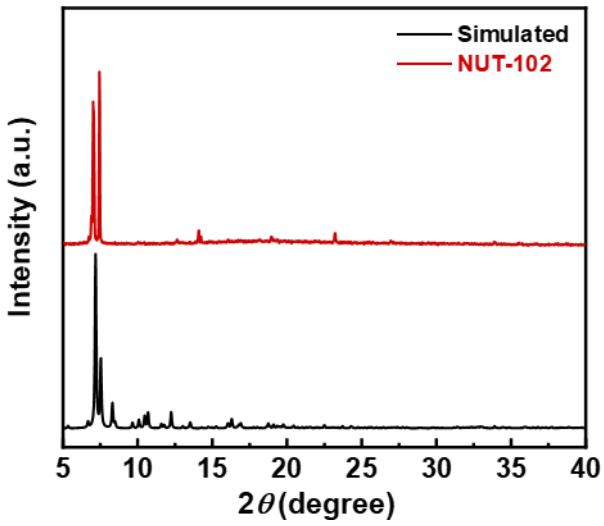

Figure S2. PXRD patterns of the simulated and as-synthesized of NUT-102.

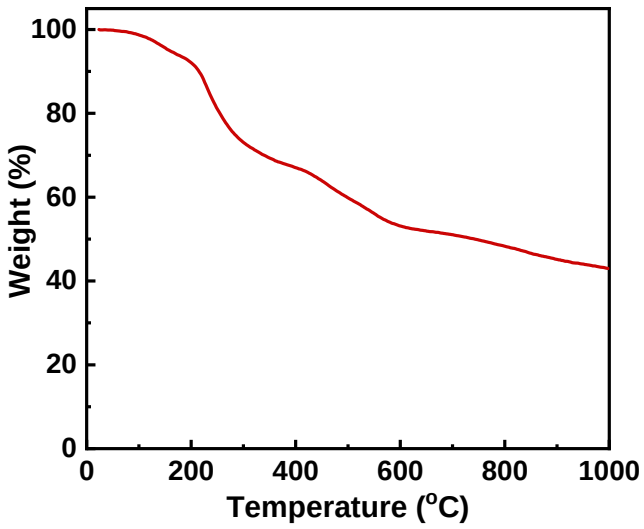

Figure S3. TGA curve of NUT-102. The high residue as observed in the TGA curve is the ZrO_2 that formed after the thermogravimetric experiment.

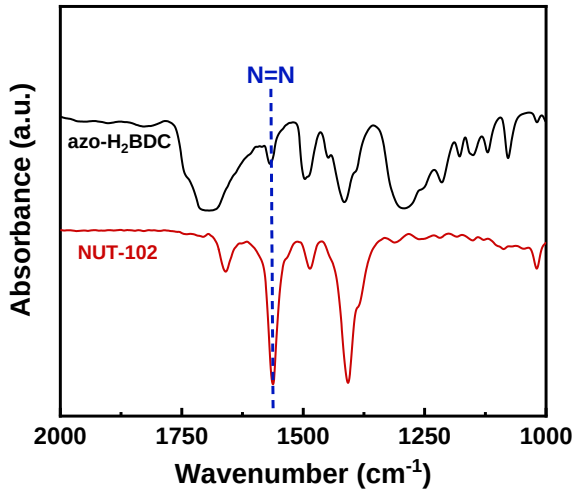

Figure S4. FTIR spectra of azo-H_2BDC and NUT-102.

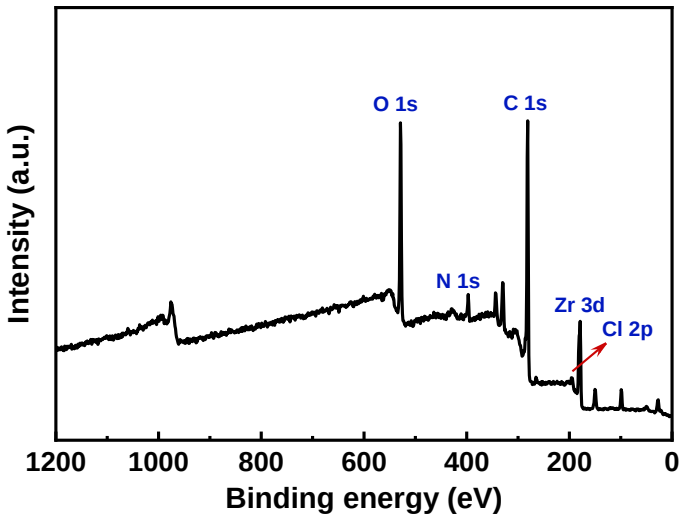

Figure S5. XPS survey spectrum of NUT-102.

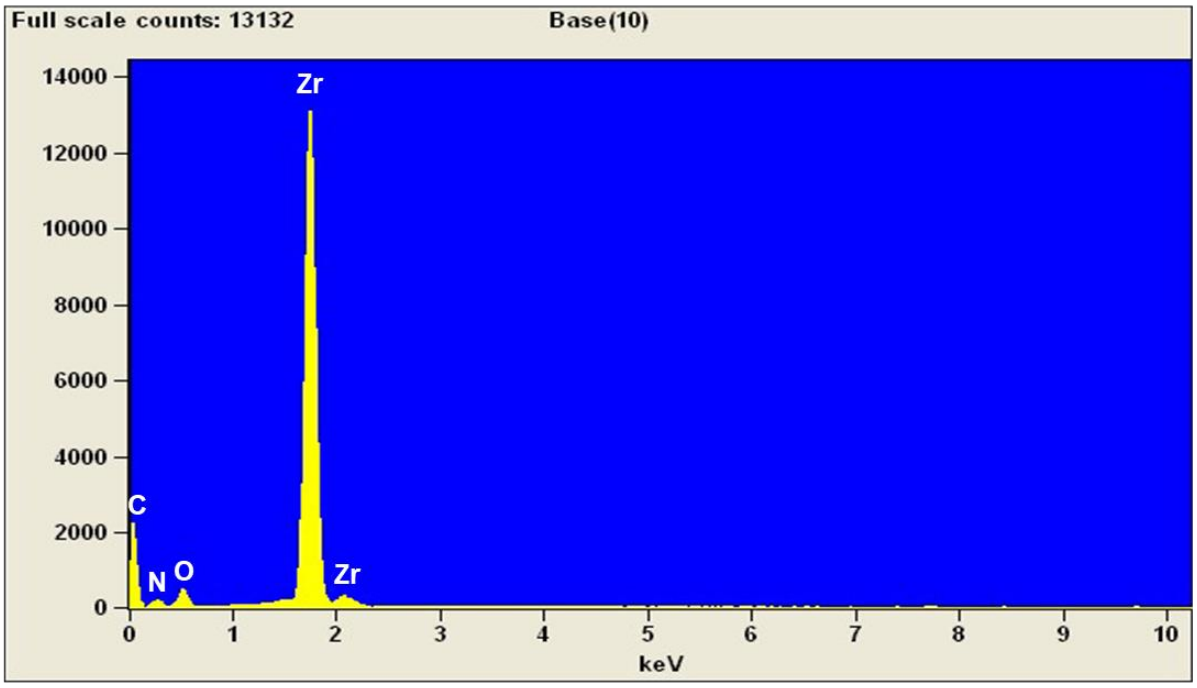

Figure S6. EDS spectrum of NUT-102.

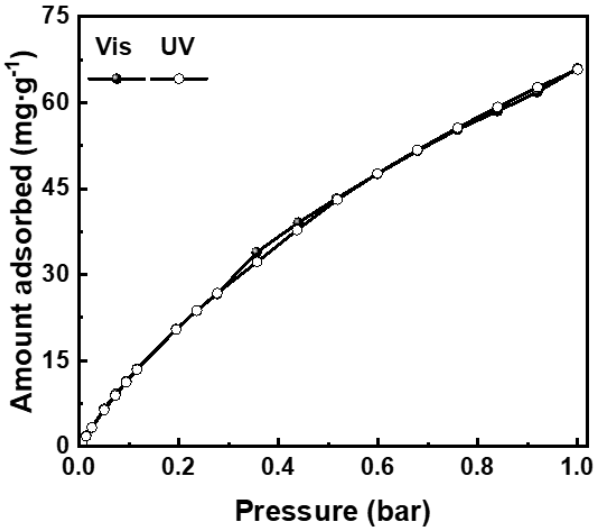

Figure S7. CO_2 adsorption isotherms of Zr-MC-1 under UV and visible light irradiation.

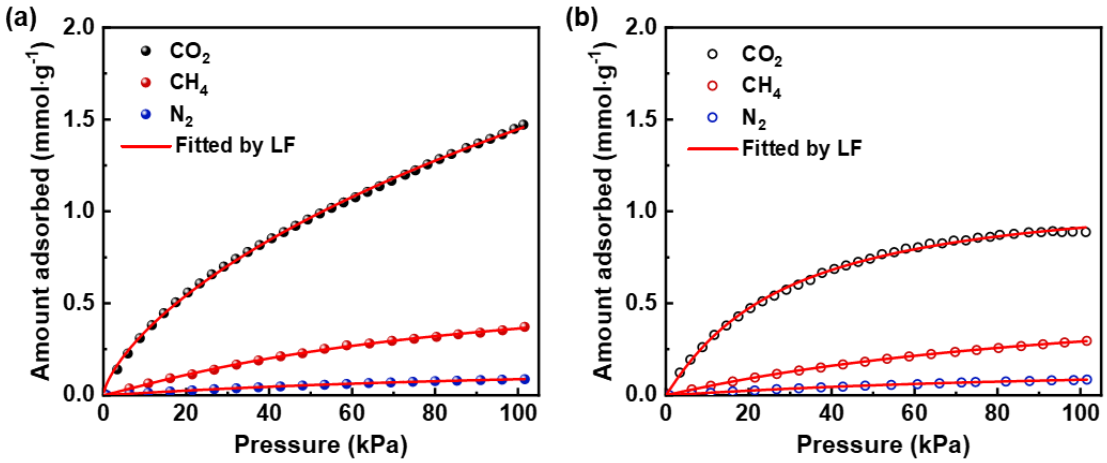

Figure S8. CO_2, CH_4, and N_2 adsorption isotherms of NUT-102 upon (a) *trans* isomerization and (b) *cis* isomerization with fitting by LF model.

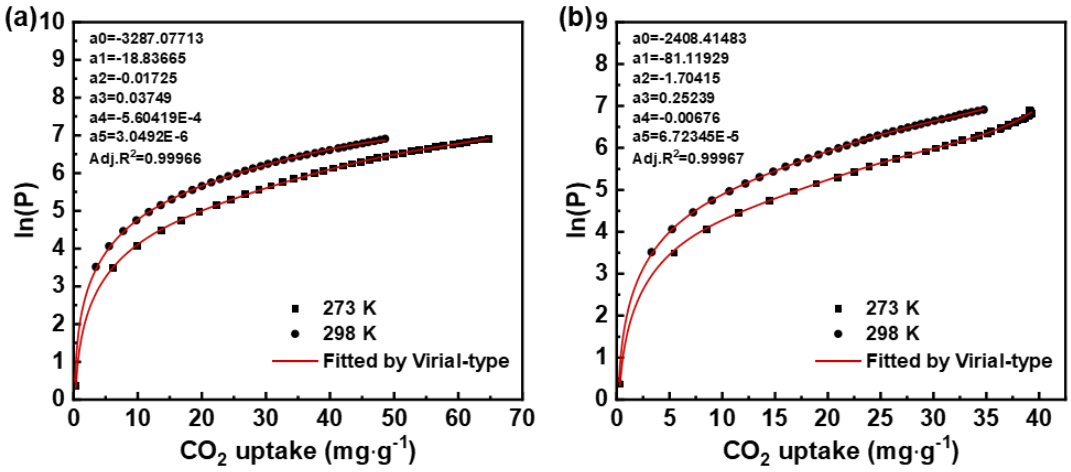

Figure S9. Global Virial fitting curves of CO_2 on NUT-102 upon (a) *trans* isomerization and (b) *cis* isomerization at different temperatures.

Table S1. Summary of crystal data and structure refinement parameters of NUT-102

Compound	NUT-102
CCDC number	2261675
Chemical formula	$C_{72}H_{52}Cl_2N_6O_{20}Zr_6$
Formula weight	1939.41
T (K)	296.15(10)
Wavelength	0.71073
Crystal system	Monoclinic
Space group	$C12/c1$
a (Å)	45.169(3)
b (Å)	14.4416(4)
c (Å)	23.9491(19)
β (°)	132.928(14)
V (Å^3)	11439(2)
Z	4
D_{calc} (mg m^{-3})	1.126
μ (mm^{-1})	0.623
F (000)	3840
θ range	1.915-25.027
Reflections collected	39149
Independent reflections	10065
R_{int}	0.1573
Completeness	0.995
Reflections observed [$I > 2\sigma$(I)]	5298
Goodness of fit on F^2	1.044
Final R indices [$I > 2\sigma$(I)]	R_1=0.1041, wR_2=0.2917
R indices (all data)	R_1=0.1495, wR_2=0.3234
Data/restrains/parameters	10065/1042/554
$\Delta\rho_{max}$, $\Delta\rho_{min}$ (e Å^{-3})	1.469, –0.886

$R_1 = \Sigma \, | |F_0| - |F_c| | / \Sigma \, |F_0|$. $wR_2 = [\Sigma w(F_0^2 - F_c^2)^2 / \Sigma w(F_0^2)^2]^{1/2}$

Table S2. The CO_2 adsorption capacity of different MOCs

MOCs	CO_2 capacity (mmol/g)	Ref.
M_8L_{12}(A)	1.003 (273 K)	5
M_8L_{12}(B)	1.005 (273 K)	5
C1$(BF_4)_4$	2.9 (298 K)	6
C1$(PF_6)_4$	1.56 (298 K)	6
C2$(BF_4)_4$	1.12 (298 K)	6
C2$(PF_6)_4$	0.85 (298 K)	6
C3$(BF_4)_4$	1.02 (298 K)	6
Zn_3(gtsp)$_3$	1.3 (298 K)	7
Cu-MOP-1	6.16 (195 K)	8
Cu-MOP-2	5.55 (195 K)	8
Cu-MOP-3	1.25 (195 K)	8
Cu_4(pdb)$_4$	3.8 (195 K)	9
Cu_4(^{t}bu-bdb)$_4$	3.5 (195 K)	9
Cu_4(tdb)$_4$	5.2 (195 K)	9
Cr_4(tdb)$_4$	3.8 (195 K)	9
Mo_4(tdb)$_4$	4.3 (195 K)	9
NUT-101	0.66 (273 K)	10
UMOP-NH_2	1.4 (298 K)	11
Zr-DBDA	0.54 (298 K)	12
b-MOP-OH	1.9 (273 K)	13
$Ni_{64}RE_{96}$	2.2 (273 K)	14
TCPB-1	0.88 (298 K)	15
NUT-102	1.47 (273 K)	This work

Table S3. Fitting parameters for the CO_2, CH_4, and N_2 adsorption isotherms of NUT-102

Sample	Gas	*Q*	*K*	*N*	R^2
trans-NUT-102	CO_2	6.89847	0.01037	0.70419	0.9995
	CH_4	0.67391	0.00721	1.10382	0.9990
	N_2	0.17917	0.00607	1.09471	0.9997
cis-NUT-102	CO_2	1.14306	0.02889	1.06624	0.9985
	CH_4	0.60921	0.00783	1.03535	0.9999
	N_2	0.16502	0.00647	1.10189	0.9991

References

1. G. M. Sheldrick, Crystal structure refinement with SHELXL, *Acta Crystallogr., Sect. C: Struct. Chem.*, 2015, **71**, 3-8.
2. G. M. Sheldrick, A short history of SHELX, *Acta Crystallogr., Sect. A: Found. Crystallogr.*, 2008, **64**, 112-122.
3. A. Spek, Single-crystal structure validation with the program PLATON, *J. Appl. Crystallogr.*, 2003, **36**, 7-13.
4. A. L. Myers and J. M. Prausnitz, Thermodynamics of mixed-gas adsorption, *AIChE J.*, 1965, **11**, 121-127.
5. J. S. Wright, A. J. Metherell, W. M. Cullen, J. R. Piper, R. Dawson and M. D. Ward, Highly selective CO_2 vs. N_2 adsorption in the cavity of a molecular coordination cage, *Chem. Commun.*, 2017, **53**, 4398-4401.
6. D. Preston, K. F. White, J. E. M. Lewis, R. A. S. Vasdev, B. F. Abrahams and J. D. Crowley, Solid-State Gas Adsorption Studies with Discrete Palladium(II) $[Pd_2(L)_4]^{4+}$ Cages, *Chem. Eur. J.*, 2017, **23**, 10559-10567.
7. B. M. Paterson, K. F. White, J. M. White, B. F. Abrahams and P. S. Donnelly, Guest-induced Assembly of Bis(thiosemicarbazonato) Zinc(II) Coordination Nanotubes, *Angew. Chem. Int. Ed.*, 2017, **56**, 8370-8374.
8. B. Doñagueda Suso, A. Legrand, C. Weetman, A. R. Kennedy, A. J. Fletcher, S. Furukawa and G. A. Craig, Porous Metal-Organic Cages Based on Rigid Bicyclo[2.2.2]oct-7-ene Type Ligands: Synthesis, Structure, and Gas Uptake Properties, *Chem. Eur. J.*, 2023, **29**, e202300732.
9. G. A. Taggart, G. R. Lorzing, M. R. Dworzak, G. P. A. Yap and E. D. Bloch, Synthesis and characterization of low-nuclearity lantern-type porous coordination cages, *Chem. Commun.*, 2020, **56**, 8924-8927.
10. Y. Jiang, P. Tan, S.-C. Qi, C. Gu, S.-S. Peng, F. Wu, X.-Q. Liu and L.-B. Sun, Breathing metal–organic polyhedra controlled by light for carbon dioxide capture and liberation, *CCS Chem.*, 2021, **3**, 1659-1668.
11. D. Nam, J. Huh, J. Lee, J. H. Kwak, H. Y. Jeong, K. Choi and W. Choe, Cross-linking Zr-based metal–organic polyhedra via postsynthetic polymerization, *Chem. Sci.*, 2017, **8**, 7765-7771.
12. X. Zhao, Y. Tang, Y. Wang, X. Rong, P. Wu, Z. Li, N. Cai, X. Deng and J. Wang, Zirconium metal–organic cage decorated with squaramides imparts dual activation for chemical fixation of CO_2 under mild conditions, *Chem. Commun.*, 2023, **59**, 10944-10947.
13. B. Lee, D. Moon and J. Park, Solvent-mediated single-crystal-to-single-crystal transformation of metal–organic cage self-assembly, *Bull. Korean Chem. Soc.*, 2023, **44**, 55-59.
14. W.-P. Chen, P.-Q. Liao, Y. Yu, Z. Zheng, X.-M. Chen and Y.-Z. Zheng, A Mixed-Ligand Approach for a Gigantic and Hollow Heterometallic Cage {Ni64RE96} for Gas Separation and Magnetic Cooling Applications, *Angew. Chem. Int. Ed.*, 2016, **55**, 9375-9379.
15. C.-X. Chen, H. Rabaâ, H. Wang, P. C. Lan, Y.-Y. Xiong, Z.-W. Wei, A. M. Al-Enizi, A. Nafady and S. Ma, In Situ Formation of Frustrated Lewis Pairs in a Zirconium Metal-Organic Cage for Sustainable CO_2 Chemical Fixation, *CCS Chem.*, 2023, **5**, 1989-1998.